TU Delft

Delft University of Technology

Document Version
Final published version

Licence
Dutch Copyright Act (Article 25fa)

Citation (APA)
Sun, P., Hu, X., Fan, J., De Bruin, E., Van Driel, W. D., & Zhang, G. (2026). Oxidation Mechanism of Copper Layer on AMB Substrate in Power Modules: A Multiscale Simulation Study. In *Proceedings - 2026 27th International Conference on Thermal, Mechanical and Multi-Physics Simulation and Experiments in Microelectronics and Microsystems, EuroSimE 2026* (Proceedings - 2026 27th International Conference on Thermal, Mechanical and Multi-Physics Simulation and Experiments in Microelectronics and Microsystems, EuroSimE 2026). IEEE. https://doi.org/10.1109/EuroSimE69483.2026.11511932

Important note
To cite this publication, please use the final published version (if applicable).
Please check the document version above.

Copyright
In case the licence states “Dutch Copyright Act (Article 25fa)”, this publication was made available Green Open Access via the TU Delft Institutional Repository pursuant to Dutch Copyright Act (Article 25fa, the Taverne amendment). This provision does not affect copyright ownership.
Unless copyright is transferred by contract or statute, it remains with the copyright holder.

Sharing and reuse
Other than for strictly personal use, it is not permitted to download, forward or distribute the text or part of it, without the consent of the author(s) and/or copyright holder(s), unless the work is under an open content license such as Creative Commons.

Takedown policy
Please contact us and provide details if you believe this document breaches copyrights.
We will remove access to the work immediately and investigate your claim.

This work is downloaded from Delft University of Technology.

2026 27th International Conference on Thermal, Mechanical and Multi-Physics Simulation and Experiments in Microelectronics and Microsystems (EuroSimE) | 979-8-3315-6249-6/26/$31.00 ©2026 IEEE | DOI: 10.1109/EuroSimE69483.2026.11511932

Oxidation Mechanism of Copper Layer on AMB Substrate in Power Modules: A Multiscale Simulation Study

Ping Sun
Electronic Components, Technology, and Materials, Department of Microelectronics
Delft University of Technology
Delft, The Netherlands
P.Sun-2@tudelft.nl

Xiao Hu
Electronic Components, Technology, and Materials, Department of Microelectronics
Delft University of Technology
Delft, The Netherlands
x.hu-1@tudelft.nl

Jiajie Fan
Electronic Components, Technology, and Materials, Department of Microelectronics
Delft University of Technology
Delft, The Netherlands
j.fan-3@tudelft.nl

Emiel de bruin
Boschman Technologies B.V.
Duiven, The Netherlands
emieldebruin@boschman.nl

Willem D. van Driel
Electronic Components, Technology, and Materials, Department of Microelectronics
Delft University of Technology
Delft, The Netherlands
willem.van.driel@signify.com

Guoqi Zhang
Electronic Components, Technology, and Materials, Department of Microelectronics
Delft University of Technology
Delft, The Netherlands
G.Q.Zhang@tudelft.nl

***Abstract*—Serving as a significant attachment component, Active Metal Brazed (AMB) substrates are prone to oxidation during storage and processing. The copper surface oxidation of AMB substrates seriously affects the reliability of high-power modules. The formation of Cu_2O/CuO oxide layer on the surface degrades interfacial qualities in subsequent packaging processes, including sintering, wire-bonding, and transfer-molding. To investigate the mechanism behind, this paper constructs a physically grounded multiscale oxidation framework that explicitly bridges molecular dynamics with reactive force field (ReaxFF-MD) and mesoscale continuum modeling. For ReaxFF-MD simulations, it aims to resolve oxygen adsorption, dissociation, diffusion behavior, and Cu–O network formation on the Cu(100), Cu(110), and Cu(111) surfaces at temperatures of 300 K and 600 K. Diffusion coefficients and interface reaction kinetic parameters are then quantitatively extracted from MD simulations and transferred as a bridge in reaction–diffusion continuum model with flux damping governed by a characteristic structural thickness. The results demonstrate that the early oxidation process of the copper surface is modulated by structural evolution and orientation anisotropy. The proposed multiscale framework provides a physical mechanism basis for understanding the early oxidation mechanism of copper and its impact on the reliability of AMB packaging.**

Keywords—AMB substrate; multi-scale oxidation coupling; ReaxFF-based MD simulation; mesoscale continuum model; FIB-SEM; EDS

I. INTRODUCTION

The continuous pursuit of higher power density, improved conversion efficiency, and elevated operating temperature in modern power electronics has imposed increasingly stringent requirements on packaging materials and interconnection technologies [1]. In particular, the rapid adoption of wide-bandgap (WBG) semiconductors such as SiC and GaN enables devices to operate at higher junction temperatures and power densities compared to conventional silicon-based systems [2]. In this case, the stability of interconnections between their constituent components in the package becomes a critical factor determining the performance and lifetime.

Among all components, AMB substrates serve as the critical foundation for interconnections, including die attachment, wire bonding, and interfacial adhesion of molding compound [3]. However, massive commercialized bare copper substrates are highly susceptible to oxidation when exposed to oxygen-containing environments during storing, transferring, or packaging processes. And the corresponding oxide layers, primarily composed of Cu_2O and/or CuO, are profoundly detrimental as they drastically compromise interfacial bonding quality in subsequent packaging steps [4, 5]. For example, surface oxidation can impair sintering quality during die attachment, reduce wire bonding strength, and weaken interfacial adhesion between molding compound and copper layer of AMB substrates. As power modules increasingly operate in demanding thermal environments, understanding copper oxidation behavior becomes essential.

From the perspective of simulation, copper oxidation is inherently a multiscale issue. At the atomic scale, MD simulations are capable of capturing atoms and molecular diffusion events and early-stage chemical reactions with high fidelity. Currently, copper early-stage oxidation [6-8] has been extensively studied with MD simulations, expanding to oxygen molecules adsorbing, dissociating, and diffusing into the copper lattice, leading to bond formation and oxide nucleation. However, this method is limited by accessible time scales (from femtoseconds to nanoseconds) and length scales (typically nanometers), making it impractical to directly predict oxide layer growth at micrometer scales relevant to engineering applications. In terms of larger scales, continuum models can describe oxide layer growth, interface migration, and morphology evolution over extended spatial and temporal domains [9, 10]. Nevertheless, these models rely heavily on phenomenological kinetic parameters, which are often obtained empirically and lack atomistic justification.

To bridge this gap, this work proposes a multiscale simulation framework that integrates ReaxFF-MD simulations and mesoscale continuum modeling to investigate

979-8-3315-6249-6/26/$31.00 ©2026 IEEE
Authorized licensed use limited to: TU Delft Library. Downloaded on July 15,2026 at 08:32:39 UTC from IEEE Xplore. Restrictions apply.

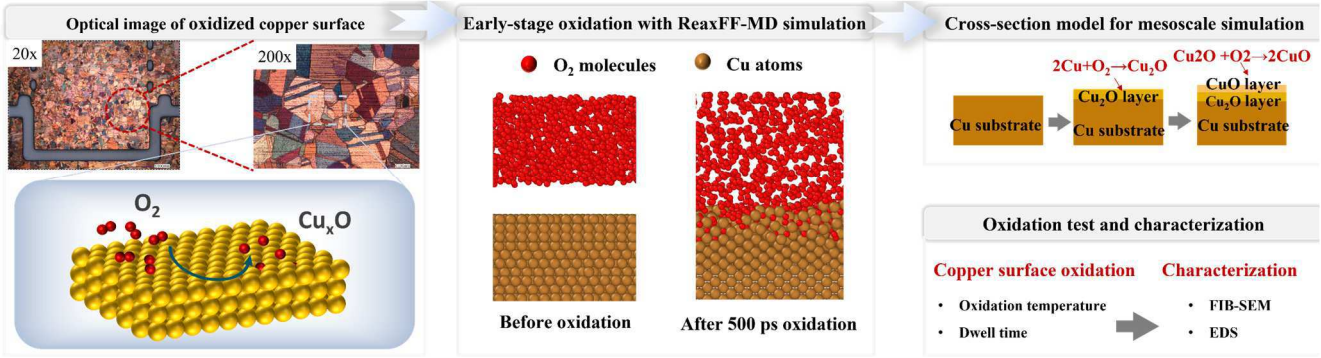


Fig. 1. Schematic diagram of oxidized copper substrate and multi-scale simulation framework.

copper surface oxidation on AMB substrates systematically. More specifically, ReaxFF-MD simulations are conducted to analyze oxygen adsorption, diffusion anisotropy, bond formation kinetics, and the oxide species evolution under varying temperatures. Key kinetic parameters, including absorption fluxes, diffusion coefficients, and reaction rates, are quantitatively extracted from MD simulation results. These bridged parameters are then subsequently incorporated into an implemented mesoscale model, which captures oxide layer growth and interface migration behavior at an extended scale. By coupling atomistic reaction mechanisms with continuum growth dynamics, this cross-scale approach enables a comprehensive understanding of copper oxidation behavior. Furthermore, AMB substrates oxidation experiments and characterizations under controlled thermal conditions are conducted to describe the oxide layer growth behaviors.

As demonstrated in Fig. 1, the proposed multiscale framework provides a physically grounded methodology for exploring oxide growth behavior and offering valuable insights on how to optimize packaging process conditions to mitigate oxidation-induced reliability risks in packaging.

II. Experimental Characterization for Motivation

Commercially bare copper AMB substrates without surface coating were used in this experiment for characterization. Firstly, bare copper samples had been stored in a controlled oxygen-containing environment (around 120000 ppm) at 300 K for six months to allow spontaneous surface oxidation. To preserve the integrity of the surface oxide layer during subsequent focused ion beam (FIB) processing [11], a thin Pt protective layer was coated on the oxidized Cu surface before cross-sectional preparation. The Pt layer effectively minimized the damage of the fragile oxide layer induced by the ion beam and possible sputtering effects.

Trenches with cross-sections were then fabricated using the FIB system. An ion beam sputtering was conducted perpendicular to the sample surface to expose the oxide/metal interface. The oxide layer thickness was measured directly from high-resolution cross-sectional SEM images, as shown in Fig. 2. And the images reveal a non-uniform oxide layer structure with a thickness of approximately 178 nm.

After FIB processing, Energy-dispersive X-ray spectroscopy (EDS) analysis was performed on the cross-section with 5 kV acceleration voltage, and Fig. 3 provides test results. The quantitative results of eZAF indicated that Cu was the main element (65.82 wt%), and the oxygen content was 0.23 wt%. It reflects the average composition of the oxide layer and the measured substrate area, rather than the pure composition of the oxide layer. Combined with the cross-sectional morphology and the stable O K peak signal, it can be confirmed that a continuous thin oxide layer has formed on the surface. The Pt M peak originated from the protective layer, whereas the trace Ga signal came from FIB processing. Combined with the cross-sectional thickness measurement results, it can be confirmed that the sample underwent low-temperature oxidation under long-term storage at 300 K.

The purpose of introducing experimental characterization in this article is to motivate the phenomenon that the AMB copper substrate undergoes oxidation in the storage environment. This is done to illustrate the real problem of engineering, rather than establishing a quantitative correspondence with the results of multiscale simulation. In other words, the experiments and simulations are carried out from mesoscale phenomena and microscale mechanisms, respectively, and they are complementary rather than mutually validating.

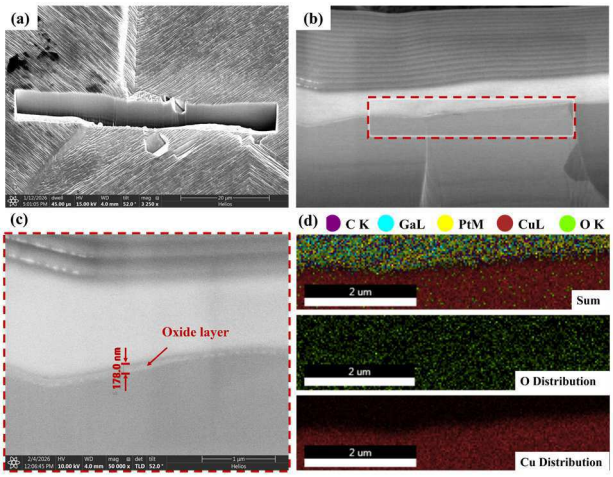


Fig. 2. Experimental characterization: (a) SEM image of the cross-sectional structure processed by FIB, (b) cross-sectional SEM image, (c) cross-sectional SEM image with oxide layer, and (d) cross-sectional element mappings.

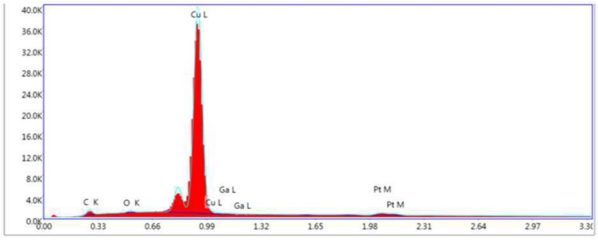


Fig. 3. The element detection results of EDS.

Authorized licensed use limited to: TU Delft Library. Downloaded on July 15,2026 at 08:32:39 UTC from IEEE Xplore. Restrictions apply.

III. Multiscale Simulation Framework

A. Reactive Molecular Dynamics Simulation

To capture the atomistic mechanisms governing early-stage copper oxidation, reactive molecular dynamics (MD) simulations were performed using a classical ReaxFF [12] for Cu–O interactions. For this study, simulations were conducted at temperatures of 300 K and 600 K using the NVT ensemble with a Nosé–Hoover thermostat. And the time step of the simulation was set to 1 fs with a time range of 500 ps to ensure numerical stability during bond formation events.

Mult-layer slab models with different surface orientations, Cu(100), Cu(110), and Cu(111), were then established to present the exposed copper layer on an AMB substrate. The simulation cell consisted of multiple atomic layers of copper, with periodic boundary conditions applied in the in-plane directions (x and y) and a free surface in the normal (z) direction. A fixed layer consisting of around five atomic layers was introduced at the bottom of the copper layers to effectively simulate the boundary constraint effect, as shown in Fig. 2. A vacuum region along the normal direction was introduced above the copper surface to provide sufficient space for oxygen molecule absorption and prevent artificial interactions between periodically repeated slabs. Oxygen molecules were randomly distributed above the copper surface with controlled initial conditions. The parameters of atomistic models with different surface orientations are listed in Table 1, including model size, the number of O_2 molecules and Cu atoms.

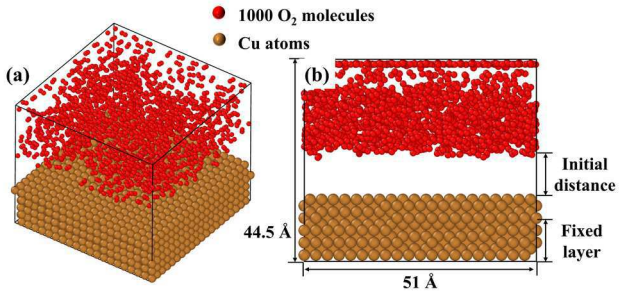
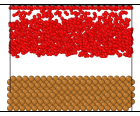
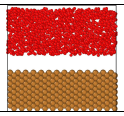
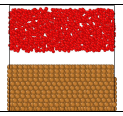


Fig. 4. Multi-layer slab model of MD simulation.

TABLE I. The Details of Atomistic Models

Details	Surface orientation of the copper layer		
	Cu (100)	Cu (110)	Cu (111)
Model			
Cu numbers	4000	3920	4800
O_2 numbers	1000		
Model size	51.12 Å*51.12 Å*44.50 Å	50.60 Å*51.12 Å*49.18 Å	51.12 Å*53.12 Å*51.56 Å
Cu layer thickness	12.23 Å	16.76 Å	12.23 Å

B. Extracted Kinetic Parameters

Although reactive MD simulations are constrained to nanosecond time scales, they provide critical quantitative parameters required for larger-scale modeling. And in the following section, these key kinetic parameters were depicted on how to extract from MD simulation results.

1) The number of chemisorbed O $N_{\text{chem O}}$ and the number of oxidized O N_{ox}, absorbed oxygen flux J, and rate of transformation k_{eff}

The chemisorbed oxygen atom was classified when the distance to any surface Cu atom was smaller than 2.2 Å, whereas the oxidized oxygen atom was defined as it coordinated with two or more Cu atoms, representing the formation of a Cu–O network structure. For the absorbed O flux, it considers the combined effect of gas-phase oxygen supply, adsorption, and capture into a quantity that can be directly used as the input of boundary flux at a larger scale:

$$J(t) = \frac{1}{A}\frac{d(N_{\text{ox}}+N_{\text{chem O}})}{dt} \tag{1}$$

While the rate of transformation reflects the adsorption-transformation kinetics of oxygen in the models:

$$k_{\text{eff}}(t) = \frac{\frac{dN_{\text{ox}}}{dt}}{N_{\text{chem O}}(t)} \tag{2}$$

2) Mean Square Displacement (MSD) and diffusion coefficient D

The mean square displacement (MSD) of oxygen atoms was computed to quantify diffusion behavior:

$$MSD(t) = \frac{1}{N}\sum_{i=1}^{N} | r_i(t) - r_i(0) |^2 \tag{3}$$

Diffusion coefficients, consisting of the normal diffusion coefficient D_z and the in-plane diffusion coefficient D_{xy}, were obtained from the slope of MSD curves:

$$D(t) = \frac{1}{2d}\frac{d\,\text{MSD}(t)}{dt} \tag{4}$$

where d is the diffusion dimension.

This distinction allows identification of diffusion anisotropy before and after oxide layer formation.

3) Activation energy

An Arrhenius-type relationship was employed using two temperatures:

$$D = D_0 \exp(-\frac{E_a}{k_B T}) \tag{5}$$

According to the diffusion coefficients at 300 K and 600 K, the activation energy was then calculated as:

$$E_a = \frac{k_B \ln(D_{300\text{K}}/D_{600\text{K}})}{\frac{1}{300\text{ K}}-\frac{1}{600\text{ K}}} \tag{6}$$

Considering only two temperatures were employed, the extracted energy should be regarded as the effective activation energy. It is primarily intended for comparative analysis between different surface orientations and diffusion directions, rather than absolute thermo-dynamic barriers.

4) Oxide Species Evolution

Using local atomic coordination analysis, the number of Cu_2O-like and CuO-like species was identified over simulation time. Within the identified oxide layer area, the effective stoichiometric ratio of the oxidation network is calculated based on Cu–O bond distance threshold (2.3 Å). On this basis, the effective stoichiometric ratio is defined as:

$$f(t) = \frac{N_{\text{ox}}(t)}{N_{\text{Cu,ox}}(t)} \tag{7}$$

Under ideal stoichiometric conditions, the ratio of Cu_2O is approximately 0.5, while that of CuO is approximately 1.

Authorized licensed use limited to: TU Delft Library. Downloaded on July 15,2026 at 08:32:39 UTC from IEEE Xplore. Restrictions apply.

C. Mesoscale Continuum Model

To extend the oxidation analysis to a larger scale, we established a mesoscale continuum model with the cross-section to represent the growing oxide layer domain and the interfaces. This model focuses on the normal diffusion, interface consumption, and average thickness evolution, excluding in-plane microstructures and defect effects.

The oxygen concentration field $c(x, y, t)$ was modeled:

$$\frac{\partial c}{\partial t} = \nabla \cdot (D_{\text{eff}} \nabla c) \tag{8}$$

Where D_{eff} is the effective oxygen diffusivity, which is directly derived from the MD-extracted normal diffusion coefficient of the diffusion-dominated stage.

h_c is essential for describing the interfacial oxidation flux damping at an extended field, and it can be extracted from MD simulation results with the following equation:

$$h_c = \frac{h_0}{\frac{J_{\text{II}}}{J_{\text{III}}} - 1} \tag{9}$$

Specifically, we divide the early stage oxidation into three stages based on the smallest total sum of squared errors for the three linear fits of the MSD curves. J_{II} is the interfacial oxidation flux at stage II, and J_{III} is the interfacial oxidation flux at stage III.

And the oxide layer growth can be expressed as:

$$\frac{dh}{dt} = \Omega_{\text{net}} J_{int}, \quad J_{int} = \frac{J_{\text{II}}}{1 + \frac{h}{h_c}} \tag{10}$$

Where J_{int} is the interfacial oxidation flux of the mesoscale model; Ω_{net} is the extracted equivalent conversion factor from interfacial oxygen consumption to geometric thickness increment. It is 0.5~1.0×10⁴ m^3/mol-O in this study.

For the upper gas-oxide layer interface:

$$c = c_g, \quad x \in \Gamma_{\text{upper}} \tag{11}$$

where c_g is the constant surface concentration, and it is determined by MD-extracted $N_{\text{chem O}}$.

For the bottom oxide layer-copper substrate interface:

$$-n \cdot (-D \nabla c) = J_{int} = k_{\text{int}} c_{\text{int}} \tag{12}$$

This mesoscopic model is used for exploring the dynamic transition trend within an extended scale. And it should be emphasized that D_{eff} was extracted from linear regression within the diffusion-dominated stage (stage II) of MD simulations. These parameters represent the average values over a short period of time. They do not stem from the parabolic oxidation law, which is applicable only on a longer time scale after the formation of a fully continuous oxide film.

IV. Results and Discussion

A. Atomistic Early-stage Oxidation Mechanism

1) Diffusion process: To reduce the influence of the initial configuration and thermal fluctuations on the statistical fluctuations during MD simulations, this study conducted three independent MD simulation calculations for the same orientations and temperature conditions. Each simulation used the same system size, ReaxFF, and thermo-dynamic control conditions, but was randomly initialized with different initial velocity distributions to ensure statistical independence.

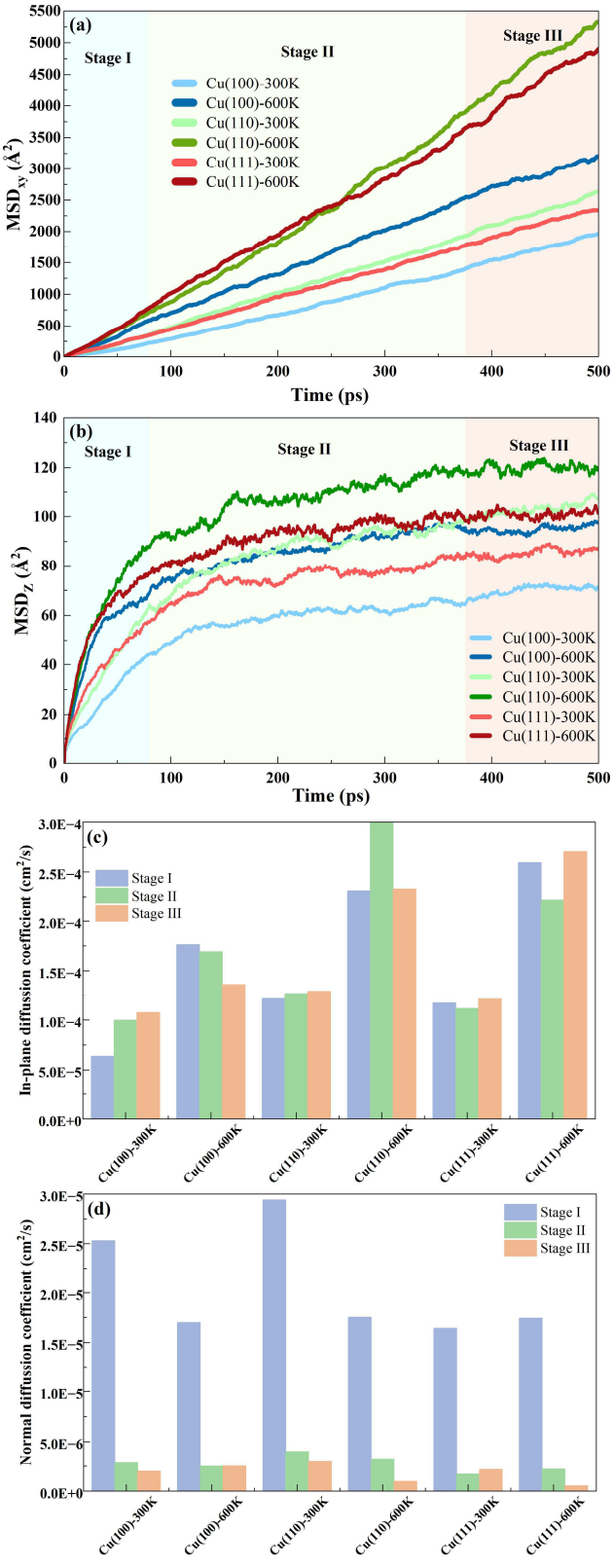


Fig. 5. Oxygen diffusion behavior description: (a) MSD_{xy} over oxidation time, (b) MSD_z over oxidation time, (c) D_{xy} over oxidation time, and (d) D_z over oxidation time. *(Three-stage mark by the system of the Cu(100) surface at 300 K)*

In terms of MSD statistics, the curves were divided into three stages to quantitatively characterize the migration behavior of oxygen atoms during the early-stage oxidation process. And then, stage-dependent effective diffusion coefficients were calculated within each stage by employing a three-segment linear model. More specifically, original MSD

Authorized licensed use limited to: TU Delft Library. Downloaded on July 15,2026 at 08:32:39 UTC from IEEE Xplore. Restrictions apply.

data is first resampled to an equal time grid of 1 ps to avoid numerical deviations caused by the output frequencies at different time steps when searching for breakpoints. Subsequently, within the condition of satisfying the minimum segment length constraint (>40 ps), two breakpoints t_1 and t_2 are exhaustively searched for, and the total sum of squared errors (SSE_{total}) of the three-segment linear regression is calculated. Finally, the breakpoint combination satisfying the smallest SSE_{total} was selected as the stage boundary time.

The system of the Cu(100) surface at 300 K is taken as a representative for the stage division result presentation, as shown in Fig. 5 (a) and (b). Stage I (0-74 ps) corresponds to the rapid normal migration process with a much larger MSD curve slope driven by the adsorption and dissociation of initial oxygen molecules. Stage II (74-376 ps) is characterized by relatively stable surface-constrained diffusion behavior with a constant diffusion coefficient, while the increased transverse diffusion can be observed. In stage III (376-500 ps), the normal MSD basically tends to a plateau, indicating that further infiltration of oxygen has been significantly restricted by the structure of the initial oxide layer within 500 ps, while lateral migration can still continue to occur in the surface or interface area. Table II provides the detailed information about the stage division.

When it comes to the effects of copper surface orientation and oxidation temperature, D_{xy} shows obvious anisotropic characteristics between different orientations. Among them, the Cu(110) and Cu(111) surfaces exhibit higher diffusion capabilities, while the diffusion of the Cu(100) surface is relatively limited. This trend is further amplified at 600 K, reflecting the synergistic regulatory effect of surface atomic structure and thermal activation on the early oxidation kinetics.

TABLE II. STAGE DIVISION UNDER DIFFERENT CONDITIONS

Condition	Stage classification (ps)		
	Stage I	***Stage II***	***Stage III***
Cu(100)-300K	0-74	74-376	376-500
Cu(100)-600K	0-165	165-426	426-500
Cu(110)-300K	0-110	110-380	380-500
Cu(110)-600K	0-211	211-425	425-500
Cu(111)-300K	0-181	181-313	313-500
Cu(111)-600K	0-166	166-361	361-500

2) Oxygen chemisorption and oxidation: This section illustrates the temporal evolution of chemisorbed oxygen and oxide oxygen on different copper surface orientations at 300 K and 600 K. These two parameters uncover the landscape of the copper early-stage oxidation kinetics, characterized by the coupling of adsorption, diffusion, and transformation processes. Moreover, the synergistic regulatory roles played by both surface orientations and temperature were performed in governing the early-stage oxidation behavior.

For the evolution of chemisorbed oxygen number, as shown in Fig. 6 (a), a clear three-stage kinetic feature is observed. Firstly, all systems exhibit a steep rise during stage I, signifying the fast adsorption and dissociation of O_2 on the copper substrates. And it is primarily governed by the rate of gas-surface collision and the density of low-coordination sites rather than by temperature. After entering Stage II, $N_{chem\ O}$ exhibits a continuous decline, and the rate of this decline is significantly enhanced at higher temperatures. This phenomenon directly indicates that the dominant mechanism has shifted from adsorption control to transformation control, where the surface-adsorbed oxygen continuously converted

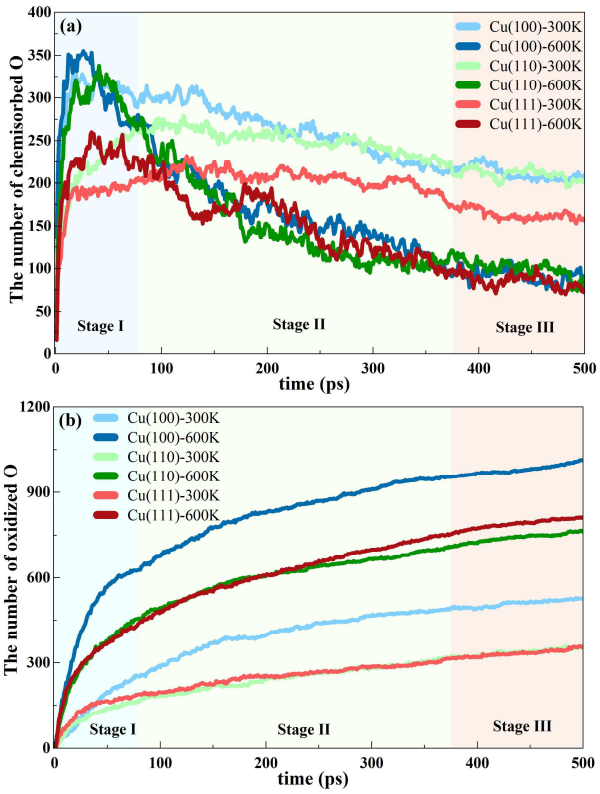


Fig. 6. Oxygen chemisorption and oxidation behavior description: (a) $N_{chem\ O}$ over oxidation time and (b) N_{ox} over oxidation time. *(Three-stage mark by the system of the Cu(100) surface at 300 K)*

into the Cu–O–Cu bridging structure and the subsurface oxygen positions, forming a stable oxide precursor network.

As shown in Fig. 6 (b), N_{ox} demonstrates a growth pattern that transitions from nearly linear to gradually decelerating over time, indicating that the oxidation process shifts from being controlled by the initial interfacial reaction to being influenced by the internal mass transfer within the oxide layer. This behavior is a typical kinetic feature in the early oxidation process of metals.

3) Oxide Layer Thickness and *Oxide Species Evolution:* Oxide layer thickness was determined by spatial distribution of oxide oxygen density along the normal direction.

For each simulation snapshot, the system was discretized into one-dimensional bins along the z-axis with a spatial resolution of 0.25 Å. The number densities of Cu and O atoms, $\rho_{Cu}(z)$ and $\rho_O(z)$, were then calculated for each bin and subsequently used to determine the local oxygen atomic fraction $x_O(z)$. The bulk Cu density was estimated from the median value of the high-density plateau region in the interior of the slab to minimize fluctuations arising from thermal vibration and local structural defects. A bin was identified as belonging to the oxide region when two criteria were simultaneously satisfied:

- $\rho_{Cu}(z) > 0.2\,\rho_{Cu,bulk}$ to ensure the presence of condensed solid phase;
- $x_O(z) > 0.05$ to indicate significant oxygen incorporation relative to metallic Cu.

Authorized licensed use limited to: TU Delft Library. Downloaded on July 15,2026 at 08:32:39 UTC from IEEE Xplore. Restrictions apply.

Among all contiguous regions satisfying these conditions, the segment located closest to the external surface was defined as the effective oxide layer. Oxide layer thickness is governed by the coupling between subsurface incorporation and interfacial structural reconstruction rather than solely by lateral diffusion capability.

$$h(t) = Max(z_{ox}) - Min(z_{ox}) \quad (13)$$

To further elucidate the growth kinetics characteristics of the early-stage oxide layer, we statistically analyzed the oxide layer thickness corresponding to different orientations and temperatures. The details of copper surface oxidation performance at 500 ps were shown in Fig. 7, and the oxide layer thickness under six conditions were summarized in Fig. 8 (a). Overall, the significant coupling effect of orientation and temperature on the early oxidation behavior of the copper surface was clearly observed.

At 300 K, the oxide layer thickness under Cu(100) is approximately 41 Å, significantly higher than 20 Å of Cu(110) and 23 Å of Cu(111), indicating that the Cu(100) surface is more conducive to the dissociation and adsorption of oxygen molecules and the rapid reconstruction of the interface. It can be explained that the regular quadruple symmetry surface of Cu(100) is more prone to form a continuous O–Cu bonding network and trigger sub-surface oxygen intercalation and structural perturbation, making the oxide layer thickness defined by density/structural threshold geometrically larger.

When the temperature rises to 600 K, the thickness of the oxide layers on Cu(110) and Cu(111) increases to approximately 23 Å and 27 Å, respectively, showing obvious thermal activation diffusion characteristics. Notably, the thickness of Cu(100) is not sensitive to temperature, further indicating that the thickness growth within this ultra-short time scale is not dominated by thermally activated bulk diffusion but rather a more interface-controlled effective kinetic process. The results show that different crystal faces during the early oxidation stage have different kinetic control mechanisms: Cu(100) is closer to interface reaction control, while Cu(110)/Cu(111) is dominated by the diffusion process. This orientation-dependent behavior provides an important basis for the subsequent modeling of cross-scale oxidation kinetics.

Fig. 8 (b) reflects that the effective stoichiometric ratio F at six conditions remained consistently within the range of 0.35–0.46 over a 500 ps phase, significantly lower than the ideal stoichiometric ratio of 0.5 for Cu_2O and much lower than 1.0 for CuO. This finding indicates that the system has not yet formed an oxygen-rich CuO structure within the current time scale. Its oxide layer should be classified as a Cu_2O-dominated structure rather than the CuO phase.

4) Activation energy: In this study, the diffusion coefficients were extracted in the diffusion-dominated stage

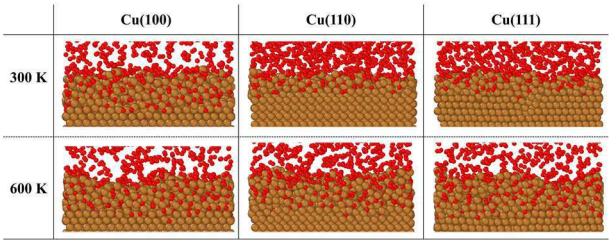


Fig. 8. Copper surface oxidations under different conditions at 500 ps.

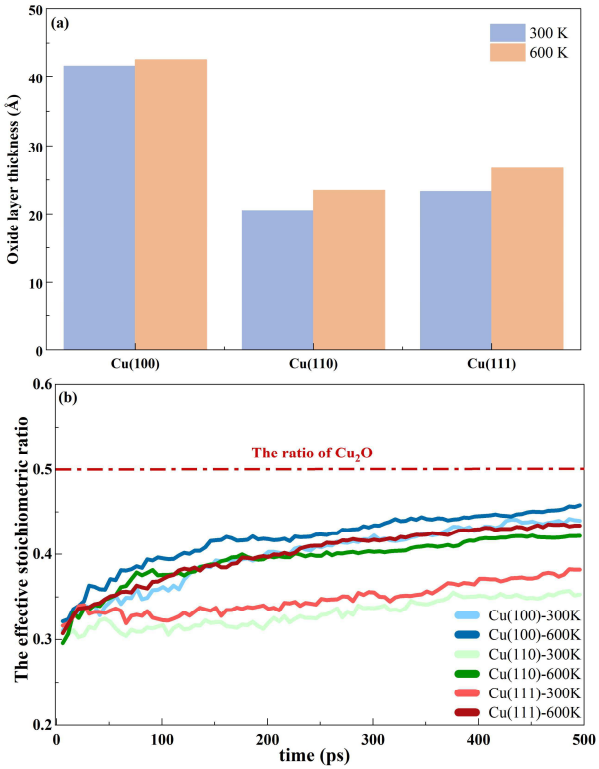


Fig. 7. The oxide layer growth: (a) oxide layer thickness at 500 ps and (b) the effective stoichiometric ratio evolution over time.

II regime using an Arrhenius-type relationship based on two temperatures. The resulting values should therefore be regarded as effective activation energy rather than thermodynamic activation energy, which are mainly used for comparative analysis between different surface orientations and diffusion directions. The activation energies for in-plane oxygen diffusion range from approximately 0.03 to 0.05 eV, indicating a weak temperature dependence and are consistent with surface-mediated or interface-mediated transport processes instead of bulk lattice diffusion during the early oxidation stage.

In contrast, the activation energies associated with normal diffusion are close to zero within numerical uncertainty. This suggests that oxygen penetration normal to the surface is not governed by a simple thermally activated hopping mechanism within the present 500 ps time window. Instead, geometric confinement, local interfacial restructuring, and short-time structural relaxation effects are likely to dominate oxygen motion in the surface-normal direction.

B. Mesoscale Oxide Layer Evolution

MD simulation captured the adsorption/dissociation of oxygen and the effective migration behavior near the interface during the early stage. Based on this, the interface oxidation flux and the effective diffusion coefficient were extracted. And these parameters were used as inputs for the mesoscale continuum model. This study constructed a reaction-diffusion mesoscale model coupling diffusion within the oxide layer and interface-level reactions to achieve mechanism extrapolation. More specifically, the interfacial oxidation flux determines the rate of oxide formation, while the migration of oxygen within the oxide layer determines the supply capacity. This coupling naturally presents a transition from reaction-limited to diffusion-limited. It should be noted that the oxide

Authorized licensed use limited to: TU Delft Library. Downloaded on July 15,2026 at 08:32:39 UTC from IEEE Xplore. Restrictions apply.

layer remains in a state of ultra-thinness at the nanometer scale, and its structure has not yet become dense or undergone significant phase transformation.

In the diffusion-dominated stage (stage II) interval, the number of oxide oxygen atoms shows a nearly linear increase, indicating that the interface reaction and oxygen supply have reached a quasi-steady-state equilibrium. In contrast, stage III includes system-level self-limiting effects such as increased oxidation layer thickness and supply limitation. Therefore, the kinetic parameters are extracted from stage II and stage III in this study. This assumption may lose validity once the oxide layer undergoes phase structure evolution. Based on the MD-extracted parameters, mesoscale oxide layer growth was simulated under different conditions using the established continuum model. Table III lists the parameters obtained through MD inversion at the 500 ps time point and the calculated thicknesses h_t at 5 ns. Several critical trends emerge from the results of mesoscale analysis.

TABLE III. PARAMETERS SUMMARY UNDER DIFFERENT CONDITIONS AND CALCULATED THICKNESSES

Condition	Parameters				
	J_{II} (mol-O/m^{-2}s^{-1})	J_{III} (mol-O/m^{-2}s^{-1})	h_c(nm)	D_{eff} (cm^2/s)	h_t (nm)
Cu(100)-300K	4.776×10^4	1.94×10^4	2.92	2.86×10^{-6}	11.62
Cu(100)-600K	6.33×10^4	3.68×10^4	5.91	2.50×10^{-6}	12.15
Cu(110)-300K	2.95×10^4	1.93×10^4	3.88	4.00×10^{-6}	7.46
Cu(110)-600K	4.72×10^4	3.57×10^4	7.29	3.28×10^{-6}	8.25
Cu(111)-300K	3.09×10^4	1.91×10^4	3.72	1.72×10^{-6}	8.31
Cu(111)-600K	6.19×10^4	3.80×10^4	2.21	2.21×10^{-6}	9.00

Firstly, temperature increase significantly enhances interfacial oxidation flux, especially reaching around 6×10^4 mol-O/m^{-2}s^{-1} for Cu(100) and Cu(111) under 600 K at the diffusion-dominated stage (stage II). And h_t shows a strong relationship with the magnitude of the interface oxidation flux. For example, the Cu(100) surface at 300 K exhibits the highest oxide layer thickness compared to that of other conditions, while the Cu(110) surface has the lowest thickness. This trend is consistent with the difference in interface oxidation capabilities, demonstrating a significant anisotropy of surface orientations.

Secondly, the response of D_{eff} to temperature does not exhibit orientation-dependent monotonicity. Cu(110) maintains the highest value at both temperatures, but slightly decreases from 300 K to 600 K; Cu(111) increases with temperature, while Cu(100) slightly decreases. It targets that the effective diffusion does not represent a physical diffusion, but is jointly regulated by the evolution of the interface structure and the connectivity of the oxidation network.

Finally, the mesoscale continuum model captures the progressive damping of interfacial flux with increasing oxide layer thickness by introducing the characteristic thickness h_c. This behavior reflects the competition between thermally accelerated interfacial reactions and structural densification within the oxide layer.

Overall, the early-stage oxidation kinetics of copper are governed predominantly by interfacial reaction processes modulated by structural evolution and orientation anisotropy, rather than by classical diffusion-controlled growth mechanisms. Specifically, these parameters should not be directly interpreted as the real reaction rate, but rather should be regarded as an effective parameter or upper limit estimate for cross-scale modeling. It is used in mesoscopic models in the form of equivalent flux or calibrated parameters to ensure physical consistency and scale self-consistency.

V. CONCLUSIONS AND OUTLOOK

This study focused on the surface oxidation issue of AMB copper substrates and constructed and analyzed a cross-scale simulation framework. The main conclusions are as follows

- The adsorption, dissociation, and migration behaviors of oxygen during the early-stage copper surface oxidation were revealed through ReaxFF-MD simulation. Based on the three-stage linear segmented method, the phased characteristics of the oxygen migration were clarified: in the initial stage, it was a rapid migration stage driven by adsorption; in the middle stage, it was a stable surface diffusion stage; and in the later stage, it was an interface-controlled stage with restricted normal migration.
- Different surface orientations exhibit significant differences in kinetics. The thickness of the oxide layer formed on the Cu(100) surface at 300 K is significantly greater than that on the Cu(110) and Cu(111) surfaces, indicating that the early growth of the oxide layer is not solely determined by the lateral diffusion ability, but is closely related to the interface reaction control mechanism.
- The effective stoichiometric ratio analysis indicates that the oxidized structure formed within the 500 ps time scale is dominated by Cu_2O, and the oxygen-rich CuO phase structure has not yet been formed.
- By extracting the diffusion coefficient and interface reaction parameters, and introducing the reaction-diffusion continuous model, the simulated reaction time was extended to 5 ns, and the mechanism exploration of the transformation trend from atomic-scale dynamics to mesoscopic-scale oxidation kinetics was achieved, demonstrating the cross-scale consistency of the transition from adsorption control to diffusion control.

In future work, to avoid the numerical instability of the traditional moving boundary method, this study aims to construct a reaction-diffusion coupling model based on the phase field method. This method can naturally capture the evolution of interface morphology and anisotropic growth behavior without showing the position of the tracking interface.

ACKNOWLEDGMENT

This work is supported by the joint project with Boschman Technologies B.V. and Electronic Components, Technology, and Materials, Department of Microelectronics, Delft University of Technology. And the authors would like to show their appreciation to Boschman Technologies B.V. for their help in sample preparation.

REFERENCES

[1] K. Wakamoto and T. Namazu, "Mechanical Characterization of Sintered Silver Materials for Power Device Packaging: A Review,"

Authorized licensed use limited to: TU Delft Library. Downloaded on July 15,2026 at 08:32:39 UTC from IEEE Xplore. Restrictions apply.

Energies, vol. 17, no. 16, pp. 4105, Aug. 2024, doi: 10.3390/en17164105.

[2] A. Athwer and A. Darwish, "A review on modular converter topologies based on WBG semiconductor devices in wind energy conversion systems," Energies, vol. 16, no. 14, pp. 5324, 2023.

[3] X. Li, L. Lin, C.-J. Du, and J. Li, "Effect of oxygen content on bonding performance of sintered silver joint on bare copper substrate," JESTPE, vol. 13, no. 3, pp. 391-398, Mar. 2023, doi: 10.1109/TCPMT.2023.3264487.

[4] X. Huang, W. He, J. Liang, H.-K. Yang, C. Zhou, and Z.-Q. Liu, "Bonding behavior and quality of pressureless Ag sintering on (111)-oriented nanotwinned Cu substrate in ambient air," Materials, vol. 17, no. 17, pp. 4423, 2024, doi: 10.3390/ma17174423.

[5] T. F. Chen and K. S. Siow, "Comparing the mechanical and thermal-electrical properties of sintered copper (Cu) and sintered silver (Ag) joints," J. Alloys Compd., vol. 866, pp. 158783, 2021, doi: 10.1016/j.jallcom.2021.158783.

[6] Y. Xia and P. Sautet, "Plasma oxidation of copper: molecular dynamics study with neural network potentials," ACS Nano, vol. 16, no. 12, pp. 20680-20692, 2022.

[7] S. J. Kim et al., "Flat-surface-assisted and self-regulated oxidation resistance of Cu (111)," Nature, vol. 603, no. 7901, pp. 434-438, 2022.

[8] X. Sun et al., "Dislocation-induced stop-and-go kinetics of interfacial transformations," Nature, vol. 607, no. 7920, pp. 708-713, 2022.

[9] M. A. Zaeem and H. El Kadiri, "An elastic phase field model for thermal oxidation of metals: Application to zirconia," Computational materials science, vol. 89, pp. 122-129, 2014.

[10] T. Q. Ansari, H. Huang, and S.-Q. Shi, "Phase field modeling for the morphological and microstructural evolution of metallic materials under environmental attack," npj Computational Materials, vol. 7, no. 1, pp. 143, 2021.

[11] J. Mayer, L. A. Giannuzzi, T. Kamino, and J. Michael, "TEM sample preparation and FIB-induced damage," MRS bulletin, vol. 32, no. 5, pp. 400-407, 2007.

[12] B. Jeon, S. K. Sankaranarayanan, A. C. Van Duin, and S. Ramanathan, "Influence of surface orientation and defects on early-stage oxidation and ultrathin oxide growth on pure copper," Philos. Mag., vol. 91, no. 32, pp. 4073-4088, 2011.

Authorized licensed use limited to: TU Delft Library. Downloaded on July 15,2026 at 08:32:39 UTC from IEEE Xplore. Restrictions apply.